Received: 14 June 2016 | Revised: 29 December 2016

DOI: 10.1002/hc.21368

RESEARCH ARTICLE

WILEY Heteroatom Chemistry

Conformational analysis of N→BH_3, N→BF_3, and N-CH_3^+ complexes with ibuprofen-derivative amides

Maria M. Romero-Chávez | **Kayim Pineda-Urbina** | **Nancy E. Magaña-Vergara** | **Rubén Vázquez-Cárdenas** | **Zeferino Gómez-Sandoval** | **Ángel Ramos-Organillo**

Facultad de Ciencias Químicas, Universidad de Colima, Coquimatlán, Colima, Mexico

Correspondence
Ángel Ramos-Organillo, Facultad de Ciencias Químicas, Universidad de Colima, Coquimatlán, Colima, Mexico.
Emails: mariaromerochavez@ucol.mx; aaramos@ucol.mx

Funding information
CONACYT-México, Grant/Award Number: #130381 and #226165

Abstract

The synthesis and structural characterization of novel amine-borane adducts of ibuprofen derivatives are presented. The changes of the electron density on the carbonyl and pyridine ring after formation of N→BH_3, N→BF_3, and N-CH_3^+ have been confirmed by ^{1}H, ^{11}B, ^{13}C, and ^{19}F NMR, further supported by homonuclear and heteronuclear correlations. Moreover, electrostatic interactions —$H^{+}\cdots{}^{-}F$ and the nonclassical $H^{+}\cdots{}^{-}H$— were identified by NMR spectra. The analysis of the resulting molecular structures offered insights on the 2-aminopyridine N→B adducts. The N→BH_3 adduct formed a single molecular arrangement, both in C_6D_6 and $CDCl_3$. The same behavior was observed for the N→BF_3 adduct in $CDCl_3$. However, two conformers of this adduct were detected in C_6D_6. All adduct geometries were corroborated by density functional theory computational calculations.

1 | INTRODUCTION

Boron's chemistry has been of interest to the scientific community due to its ability to form homonuclear bonds and coordinate to electron-rich atoms, for example, nitrogen, oxygen, sulfur, and phosphorus.[1,2] Organoboron compounds are characterized by hydroxyl-boron and amine-boron interactions and are important in many biological processes, for example, calcium and insulin metabolism, growth and maintenance of bones, and some cell signaling mechanisms.[3–10] Also, these compounds have been applied as reagents in organometallic and supramolecular chemistry,[11] and as polymer precursors,[12] reducing agents,[13] catalysts,[14,15] luminescent materials,[16] and hydrogen storage.[17,18]

Boron's interactions with the elements of group 15 are classic examples of reactions between Lewis acids and bases. The vacant *p* orbital, on the boron atom, is a strong p-electron acceptor. For example, the N→B interaction shows some advantages over a C-C bond, like the reversibility of the formed adduct and its bond strength, both of which are influenced by the functionalization of the boron and nitrogen atoms.[11]

Differences between N→B adducts and N-C bonds have also been studied on a range of structures with dithiazinane, ethanolamine, imine, and imidazole derivatives, where the electronic properties of nitrogen atom are affected by the possibility to share its free electron pair.[19,20] This lone electron pair gives way to discuss an isolobal analogy, which has been observed in amino-aluminum and amino-boron complexes before.[21]

Aminopyridines are systems with two nitrogen atoms with sp^2 and sp^3 hybridization, where the amine group makes the pyridine nitrogen more basic than a pyridine's nitrogen. Their chemical reactivity depends on the pyridine nitrogen position with respect to the amine group.[22] Aminopyridines coupled to ibuprofen have been studied for their participation in the process of neutrophil chemotaxis, where the amide derivatives of 2-aminopyridine show a better activity compared to those derived from 3- and 4-aminopyridine.[23]

Dissolved molecular systems' intramolecular and intermolecular interactions are affected by the solvent's polarity; polar solvents tend to favor electrostatic interactions, while

Contract grant sponsor: CONACYT-México.

Contract grant number: #130381, #226165.

nonpolar solvents have a weakening effect on Van der Waals interactions. Besides any interactions with the medium, amine-borane adducts exhibit other noncovalent interactions, like N-$H^{\delta+}$…$^{-\delta}$H-B, which underscore their binding with biomolecules. Furthermore, these hydride-proton interactions can benefit the structure stability.[24–26]

This work reports the synthesis and structural analysis of aminopyridines derived from a racemic mixture of ibuprofen, as well as the formation of N→B adducts under different experimental conditions. The results of NMR analysis demonstrate the presence of different structural conformers formed by the electronic effect of the lone pair of nitrogen atom when it form adducts with BH_3 and BF_3 or covalent bonds with -CH_3 in $CDCl_3$ and C_6D_6. In addition, Density Functional Theory calculations were performed to further explain the proposed structures for the adducts by the analysis of NMR spectra, where N→BF_3 adduct in C_6D_6 showed two different conformers as well.

2 | EXPERIMENTAL

2.1 | General information

Ibuprofen was supplied by the Alfadelta S. A. de C. V. as racemic mixture and it was not further purified. Other reagents were obtained from Sigma-Aldrich, USA, and they were used without further purification. Thin-layer chromatography (TLC) was run on silica gel (60Å) (Sigma-Aldrich). The NMR spectra were obtained by dissolving compounds in $CDCl_3$ or C_6D_6 and analyzed with a Bruker 400 MHz NMR spectrometer for ^{1}H (400.13 247 MHz), ^{13}C (100.62 282 MHz), ^{11}B (128.37 760 MHz), and ^{19}F (376.46 071 MHz). NMR of ^{15}N was obtained by INEPT and HSQC with NH_4NO_3 utilized as reference (δ=0.0 ppm), where only the amide nitrogen was observed. Chemical shifts (δ) are reported in ppm and coupling constants in Hz (see Supporting Information). The infrared spectra were recorded on a Varian Excalibur 3100 FT-IR spectrophotometer using KBr pellets. Elemental analyses were performed on Truspec Micro elemental analyzer.

2.2 | General procedure for the synthesis of ibuprofen bencenacetamides 1-3

The amides (Scheme 1) used for the formation of N→BH_3, N→BF_3, adducts and N-CH_3^+ bond were obtained following the reported method by Faisal MM and Najeh AH[27] There, the carbonyl group is activated by forming an ester intermediate with *N,N′*-Dicyclohexylcarbodiimide (DCC) in the presence of 4-Dimethylaminopyridine (DMAP) which is acting as catalyst. These systems were reported by Cocco MT et al. with other synthesis procedures.[28]

In a dry ball flask, the ibuprofen (1000 mg, 4.84 mmol), aminopyridine (1000 mg, 4.84 mmol), DMAP (60 mg, 0.5 mmol), and dry THF (100 mL) were mixed at room temperature. This was followed by the dropwise addition of DCC (1000 mg, 4.84 mmol) during 15 minutes at 0°C. The reaction was left stirring at room temperature overnight. A precipitated solid—dicyclohexylurea (DCU)— was filtered, and the solvent was evaporated under reduced pressure. The sample was left in ethyl acetate at 5°C for 24 hours, after which a precipitated solid was removed by filtration and the solvent was evaporated under reduced pressure. The amides were purified by column chromatography with a mixture of hexane:ethyl acetate, 4:1 ratio for **1** and **2,** and 1:1 ratio for **3**.

2.2.1 | 2-[4-(2-methylpropyl)phenyl]-N-(pyridin-2-yl)propanamide (1)

Yellow, wax-like product, 90% yield. ^{1}H NMR (400 MHz, $CDCl_3$) δ 8.25 (s, 1H, -N*H*), 8.22 (d, ^{3}J=8.4 Hz, 1H, H14), 8.14 (m, 1H, H17), 7.21 (d, ^{3}J=7.7 Hz, 1H, H2), 7.21 (d, ^{3}J=7.7 Hz, 1H, H6), 7.17 (d, ^{3}J=8.0 Hz, 1H, H3), 7.17 (d, ^{3}J=8.0 Hz, 1H, H5), 7.13 (ddd, ^{3}J=1.8 Hz, ^{3}J=1.8 Hz,

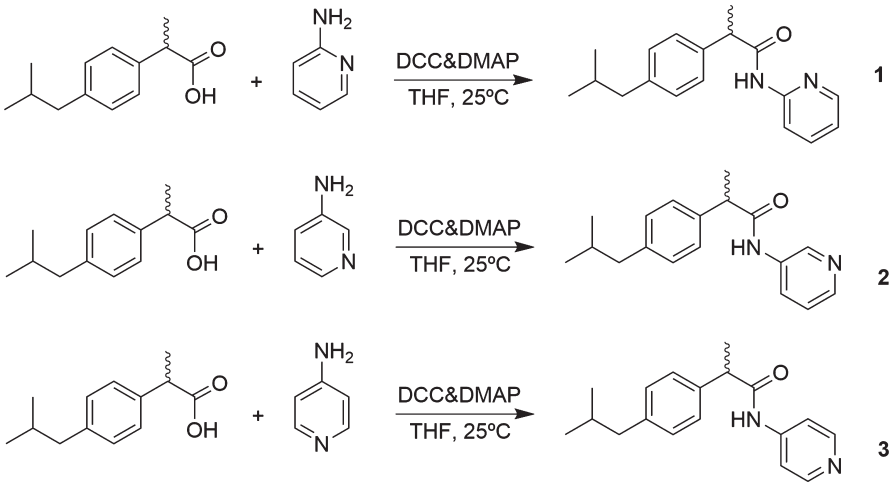

SCHEME 1 Synthetic pathway of **1-3** amides ibuprofen derivatives

^{4}J=0.5 Hz, 1H, H15), 6.13 (m, 1H, H16), 3.64 (q, ^{3}J=7.2 Hz, 1H, H7), 2.45 (d, ^{3}J=7.1 Hz, 2H, H9), 1.84 (m, 1H, H10), 1.53 (d, ^{3}J=7.1 Hz, 3H, H8), 0.81 (d, ^{3}J=6.6 Hz, 6H,11H). ^{15}N NMR (400 MHz, $CDCl_3$) δ 141.3 (-NH). ^{13}C NMR δ (400 MHz, $CDCl_3$) δ 173.1 (C12), 151.4 (C13), 146.1 (C17), 141.0 (C4), 139.7 (C1), 139.3 (C15), 129.8 (C2, C6), 127.2 (C3, C5), 119.4 (C16), 114.1 (C14), 47.9 (C7), 45.2 (C9), 30.1 (C10), 22.7 (C11), 17.8 (C8).

2.2.2 | 2-[4-(2-methylpropyl)phenyl]-N-(pyridin-3-yl)propanamide (2)

Brown, wax-like product, 88% yield. ^{1}H NMR (400 MHz, $CDCl_3$) δ 8.09 (s, 1H, H14), 8.53 (s, 1H, -NH), 8.22 (d, ^{3}J=4.5 Hz, 1H, H17), 8.11 (d, ^{3}J=8.5 Hz, 1H, H15), 7.31 (d, ^{3}J=8.0 Hz, 1H, H2), 7.16 (d, ^{3}J=7.9 Hz, 1H, H3), 7.16 (d, ^{3}J=7.9 Hz, 1H, H5), 7.16 (d, ^{3}J=8.0 Hz, 1H, H6), 7.10 (m, 1H, H16), 3.74 (q, ^{3}J=7.0 Hz 1H, H7), 2.56 (d, ^{3}J=8.5 Hz, 2H, H9), 1.86 (m, 1H, H10), 1.64 (d, ^{3}J=7.1 Hz, 3H, H8), 0.92 (d, ^{3}J=6.6 Hz, 6H, H11). ^{15}N NMR (400 MHz, $CDCl_3$) δ 125.2 (-NH). ^{13}C NMR (400 MHz, $CDCl_3$) δ 173.6 (C12), 144.4 (C17), 141.2 (C14), 140.7 (C4), 137.9 (C1), 135.3 (C13), 129.8 (C2, C6), 127.5 (C3, C5), 127.5 (C15), 123.7 (C16), 47.5 (C7), 45.0 (C9), 30.2 (C10), 22.4 (C11), 18.6 (C8).

2.2.3 | 2-[4-(2-methylpropyl)phenyl]-N-(pyridin-4-yl)propanamide (3)

Yellow, wax-like product, 93% yield. ^{1}H NMR (400 MHz, $CDCl_3$) δ 8.43 (s, 1H, -NH), 8.36 (d, ^{3}J=5.5 Hz, 1H, 15H), 8.36 (d, ^{3}J=5.5 Hz, 1H, H16), 7.51 (d, ^{3}J=5.8 Hz, 1H, H14), 7.51 (d, ^{3}J=5.8 Hz, 1H, H17), 7.22 (d, ^{3}J=8.0 Hz, 1H, H2), 7.16 (d, ^{3}J=8.0 Hz, 1H, H3), 7.16 (d, ^{3}J=8.0 Hz, 1H, H5), 7.16 (d, ^{3}J=8.0 Hz, 1H, H6), 3.67 (q, ^{3}J=7.0 Hz, 1H, H7), 2.53 (d, ^{3}J=7.2 Hz, 2H, H9), 1.87 (m, ^{3}J=6.7 Hz, 1H, H10), 1.51 (d, ^{3}J=7.0 Hz, 3H, H8), 0.91 (d, ^{3}J=6.6 Hz, 6H, H11). ^{15}N NMR (400 MHz, $CDCl_3$) δ 137.2 (-NH). ^{13}C NMR (400 MHz, $CDCl_3$) δ 174.0 (C12), 149.6 (C15, C16), 146.2 (C13), 141.1 (C4), 137.7 (C1), 129.8 (C2, C6), 127.5 (C3, C5), 113.8 (C14, C17), 47.6 (C7), 45.0 (C9), 30.1 (C10), 22.4 (C11), 18.7 (C8).

2.3 | Synthesis of adducts N→Boron with BH_3, BF_3, and CH_3I

The synthesis of **1a-3a** and **1b-3b** adducts was carried out under the same conditions of time and temperature, varying only the type of deuterated solvent ($CDCl_3$ and C_6D_6) to find structural differences (Scheme 2).

1a-3a and **1b-3b** were synthesized following the Schlenk technique under a nitrogen atmosphere. For **1a-3a,** boron trifluoride diethyl etherate ($Et_2O{\cdot}BF_3$) (0.22 mL, 1.77 mmol) was added to 5 mL of the corresponding amide (0.50 g, 1.77 mmol) solution in dry $CHCl_3$ in an ice bath (*Method i*).

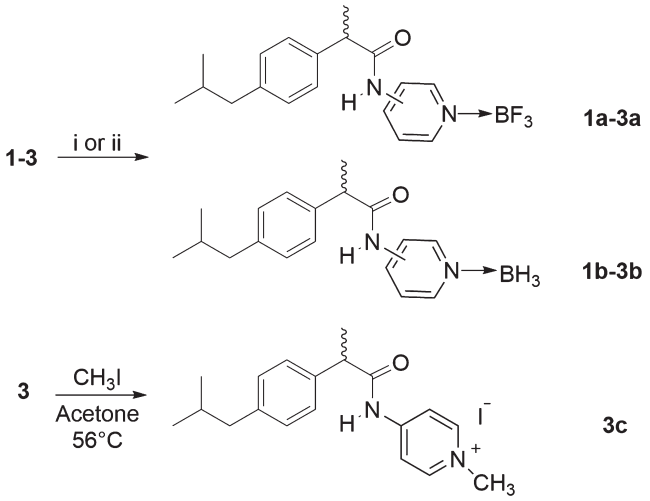

SCHEME 2 Synthesis of N→BH_3, N→BF_3 adducts (i: $CDCl_3$, $Et_2O{\cdot}BF_3$, or DMS·BH_3; ii: C_6D_6, $Et_2O{\cdot}BF_3$ or DMS·BH_3) and N-CH_3 + salt with ibuprofen-derived amides

For **1b-3b**, $Et_2O{\cdot}BF_3$ was substituted by borane dimethyl sulfide complex (DMS·BH_3) (0.17 mL, 1.77 mmol) following the above method. The products were isolated by vacuum-assisted solvent evaporation and were immediately analyzed by FT-IR and elemental analysis. The resulting compounds had tendency to react with the ambient humidity, effectively destroying the N→B interaction.

To make their NMR analysis viable, the products were synthesized inside a NMR tube. The synthesis followed the previously described method, substituting the $CHCl_3$ for $CDCl_3$ and downscaling the used quantities from 1.77 mmol to 0.18 mmol. In addition, the adducts were also synthesized using C_6D_6 as solvent to explore the solvent effect on the structure (*Method ii*).

The synthesis of **3c** followed the next process. Methyl iodide (0.28 mL, 4.42 mmol) was added to 5 mL of an amide **3** (0.5 g, 1.77 mmol) solution in acetone. The reaction was left 12 h to reflux. This was followed by the removal of the solvent and the excess of CH_3I by vacuum-assisted evaporation. The aromatic nitrogen methylation was carried out only for the amide **3**, as the methylation for amides **1** and **2** failed in all of the conditions presented in Table 1.[29–31]

2.3.1 | Trifluoro(2-(2-(4-isobutylphenyl) propanamido)pyridin-1-ium-1-yl)borate (1a*)

Yellow sticky wax-like product, 88% yield. ^{1}H NMR (400 MHz, $CDCl_3$) δ 10.24 (s, 1H, -NH), 8.21 (d, ^{3}J=8.8 Hz, 1H, H14), 8.16 (m, 1H, H17), 7.56 (dd, ^{3}J=6.1 Hz, ^{3}J=6.1 Hz, 1H, H15), 7.38 (m, 1H, H16), 7.24 (d, ^{3}J=7.9 Hz, 1H, H2), 7.24 (d, ^{3}J=8.1 Hz, 1H, H6), 6.97 (d, ^{3}J=8.1 Hz, 1H, H3), 6.97 (d, ^{3}J=8.1 Hz, 1H, H5), 3.93 (q, ^{3}J=7.1 Hz, 1H, H7), 2.31 (d, ^{3}J=7.2 Hz, 2H, H9), 1.71 (m, 1H, H10), 1.45 (d, ^{3}J=7.0 Hz, 3H, H8), 0.72 (d, ^{3}J=6.6 Hz, 6H, H11). ^{15}N (400 MHz, $CDCl_3$)

TABLE 1 Reaction conditions tested for methylation

Amide	CH_3I	Solvent	Time/Temperature	Product
1 eq	2.5 eq	Acetone	4 h in reflux	**3c**
1 eq	4 eq	Acetone	18 h in reflux	N/A
1 eq	4 eq	Toluene	4 h in reflux	N/A
1 eq	4 eq	Ethanol	1 h on ice, then 72 h at room temperature	N/A
1 eq	4 eq	Ethanol	1 h on ice, then 12 h in reflux	N/A

N/A, not available.

δ 131.9 (-NH). ^{13}C NMR (400 MHz, $CDCl_3$) δ 178.8 (C12), 148.4 (C13), 147.1 (C17), 141.4 (C4), 139.8 (C1), 136.8 (C15), 130.0 (C2, C6), 129.2 (C3, C5), 121.0 (C16), 116.8 (C14), 46.9 (C7), 45.2 (C9), 30.1 (C10), 22.6 (C11), 18.4 (C8). ^{11}B NMR (400 MHz, $CDCl_3$) δ −1.0. ^{19}F NMR (400 MHz, $CDCl_3$) δ −147.8. Anal. ($C_{18}H_{22}N_2O$ BF_3): Calcd. C, 61.74; H, 6.33; B, 3.09; F, 16.28; N, 8.00; O, 4.57; found: C, 61.39; H, 6.29; N, 7.95. (*for cyclic conformer).

2.3.2 | (2-(2-(4-isobutylphenyl) propanamido)pyridin-1-ium-1-yl) trihydroborate (1b*)

Colorless sticky wax-like product, 80% yield. ^{1}H NMR (400 MHz, $CDCl_3$) δ 9.28 (s, 1H, -NH), 8.51 (d, ^3J=8.6 Hz, 1H, H14), 8.28 (d, ^3J=5.8 Hz, 1H, H17) 7.82 (dd, ^3J=7.8 Hz, ^3J=7.8 Hz,1H, H15), 7.31 (d, ^3J=7.9 Hz, 1H, H2), 7.31 (d, ^3J=8.1 Hz, 1H, H6), 7.08 (d, ^3J=8.1 Hz, 1H, H3), 7.08 (d, ^3J=8.1 Hz, 1H, H5), 7.02 (m, 1H, H16), 3.55 (q, ^3J=7.1 Hz, 1H, H7), 2.39 (d, ^3J=7.3 Hz, 2H, H9), 1.82 (m, 1H, H10), 1.56 (d, ^3J=7.0 Hz, 3H, H8), 0.82 (d, ^3J=6.5 Hz, 6H, H11). ^{15}N NMR (400 MHz, $CDCl_3$) δ 136.8 (-NH). ^{13}C NMR (400 MHz, $CDCl_3$) δ 172.9 (C12), 148.8 (C13), 146.5 (C17), 141.5 (C4), 141.5 (C15), 136.5 (C1), 130.0 (C2, C6), 127.5 (C3, C5), 118.8 (C16), 115.5 (C14), 48.4 (C7), 45.0 (C9), 30.2 (C10), 25.8 (C11), 22.3 (C8). ^{13}C NMR (400 MHz, $CDCl_3$) δ −20.2 (q, $^1J_{(B\text{-}H)}$=105.5 Hz, -BH_3). Anal. (C_{18} $C_{18}H_{22}N_2OBH_3$): Calcd. C, 72.99; H, 8.51; B, 3.65; N, 9.46; O, 5.40; found C, 72.43; H, 8.42; N, 9.36.

2.3.3 | 1-(difluoroboryl)-3-(2-(4-isobutylphenyl)propanamido)pyridin-1-ium fluoride (2a)

Yellow sticky wax-like product, 82% yield. ^{1}H NMR (400 MHz, $CDCl_3$) δ 9.11 (s, 1H, -NH), 9.11 (d, ^3J=5.1 Hz, 1H, H14), 8.47 (d, ^3J=7.7 Hz, 1H, H17), 8.27 (m, 1H, H15), 7.78 (m, 1H, H16), 7.27 (d, ^3J=8.3 Hz, 1H, H2), 7.27 (d, ^3J=8.3 Hz, 1H, H6), 7.01 (d, ^3J=7.6 Hz, 1H, H3), 7.01 (d, ^3J=7.6 Hz, 1H, H5), 3.87 (m, 1H, 7H), 2.32 (d,^3J=6.2 Hz, 2H, H9), 1.89 (m, 1H, 10H), 1.48 (d, ^3J=6.1 Hz, 3H, H8), 0.81 (d, ^3J=6.4 Hz, 6H, H11). ^{15}N NMR (400 MHz, $CDCl_3$) δ 126.3 (-NH). ^{13}C NMR (400 MHz, $CDCl_3$) δ 175.7 (C12), 141.1 (C4), 137.0 (C1), 136.9 (C14), 136.5 (C15), 136.2 (C13), 132.5 (C16), 129.7 (C2, C6), 127.5 (C3, C5), 127.7 (C17), 46.9 (C7), 45.0 (C9), 30.1 (C10), 22.3 (C11), 18.2 (C8). ^{11}B NMR (400 MHz, $CDCl_3$) δ −0.8. ^{19}F NMR (400 MHz, $CDCl_3$) δ −147.3. Anal. ($C_{18}H_{22}N_2OBF_3$): Calcd. C, 61.74; H, 6.33; B, 3.09; F, 16.28; N, 8.00; O, 4.57; found C, 61.35; H 6.27; N 7.70.

2.3.4 | (3-(2-(4-isobutylphenyl) propanamido)pyridin-1-ium-1-yl) trihydroborate (2b)

Colorless sticky wax-like product, 78% yield. ^{1}H NMR (400 MHz, $CDCl_3$) δ 8.60 (s, 1H, H14), 8.34 (d, ^3J=8.3 Hz, 1H, H15), 8.23 (d, ^3J=5.0 Hz, 1H, H17), 8.05 (s, 1H, -NH), 7.39 (m, 1H, H16), 7.28 (d, ^3J=7.9 Hz, 1H, H2), 7.28 (d, ^3J=7.9 Hz, 1H, H6), 7.05 (d, ^3J=7.8 Hz, 1H, H3), 7.05 (d, ^3J=7.8 Hz, 1H, H5), 3.71 (q, ^3J=7.1 Hz, 1H, H7), 2.37 (d, ^3J=7.1 Hz, 2H, H9), 1.83 (m, 1H, H10), 1.48 (d, ^3J=7.0 Hz, 3H, H8), 0.88 (d, ^3J=6.5 Hz, 6H, H11). ^{15}N NMR (400 MHz, $CDCl_3$) δ 124.6 (-NH). ^{13}C NMR (400 MHz, $CDCl_3$) δ 173.5 (C12), 142.2 (C17), 141.4 (C4), 138.7 (C14), 137.0 (C1), 136.9 (C13), 129.4 (C15), 129.9 (C2, C6), 127.3 (C3, C5), 125.4 (C16), 47.5 (C7), 45.0 (C9), 30.1 (C10), 22.9 (C11), 18.5 (C8). ^{11}B NMR (400 MHz, $CDCl_3$) δ −20.3 (q, $^1J_{(B\text{-}H)}$=106.3 Hz, -BH_3). Anal. ($C_{18}H_{22}N_2OBH_3$): Calcd. C, 72.99; H, 8.51; B, 3.65; N, 9.46; O, 5.40; found C, 72.94; H, 8.36; N, 9.30.

2.3.5 | 1-(difluoroboryl)-4-(2-(4-isobutylphenyl)propanamido)pyridin-1-ium fluoride (3a)

Yellow sticky wax-like product, 78% yield. ^{1}H NMR (400 MHz, $CDCl_3$) δ 9.31 (s, 1H, -NH), 8.27 (d,^3J= 5.9 Hz, 1H, H16), 8.27 (d, ^3J= 5.9 Hz, 1H, H15), 8.01 (d, ^3J= 6.2 Hz, 1H, H17), 8.01 (d, ^3J= 6.2 Hz, 1H, H14), 7.28 (d, ^3J= 7.2 Hz, 1H, H2), 7.28 (d, ^3J= 7.2 Hz, 1H, H6), 7.04 (d, ^3J= 8.0 Hz, 1H, H5), 7.04 (d, ^3J=8.0 Hz, 1H, H3), 3.88 (q, ^3J= 6.8 Hz, 1H, H7), 2.36 (d, ^3J= 7.1 Hz, 2H, H9), 1.76 (m, 1H, H10), 1.52 (d, ^3J= 7.0 Hz, 3H, H8), 0.87 (d, ^3J= 6.6 Hz, 6H, H11). ^{15}N NMR (400 MHz, $CDCl_3$) δ 137.9 (-NH). ^{13}C NMR

(400 MHz, $CDCl_3$) δ 174.0 (C12), 153.8 (C15, C16), 141.8 (C13), 141.7 (C4), 137.4 (C1), 129.9 (C2, C6), 127.4 (C3, C5), 115.0 (C14, C17), 47.8 (C7), 18.1 (C8), 45.1 (C9), 30.1 (C10), 22.3 (C11). ^{11}B NMR (400 MHz, $CDCl_3$) δ −0.9. ^{19}F NMR (400 MHz, $CDCl_3$) δ −147.2. Anal. ($C_{18}H_{22}N_2O\,BF_3$): Calcd. C, 61.74; H, 6.33; B, 3.09; F, 16.28; N, 8.00; O, 4.57; found C, 61.52; H, 6.79; N, 8.04.

2.3.6 | (4-(2-(4-isobutylphenyl) propanamido)pyridin-1-ium-1-yl) trihydroborate (3b)

Colorless sticky wax-like product, 85% yield. ^{1}H NMR (400 MHz, $CDCl_3$) δ 8.24 (s, 1H, -NH), 8.29 (d, ^3J=7.0 Hz, 1H, H16), 8.29 (d,^3J=7.1 Hz, 1H, H15), 7.62 (d, ^3J=7.0 Hz, 1H, H17), 7.62 (d, ^3J=7.0 Hz, 1H, H14), 7.22 (d, ^3J=8.0 Hz, 1H, H6), 7.22 (d, ^3J=8.0 Hz, 1H, H2), 7.13 (d, ^3J= 8.0 Hz, 1H, H5), 7.13 (d, ^3J=8.0 Hz, 1H, H3), 3.80 (q, ^3J=7.0 Hz, 1H, H7), 2.43 (d,^3J=7.2 Hz, 2H, H9), 1.84 (m, 1H, H10), 1.55 (d, ^3J=7.0 Hz, 3H, H8), 0.90 (d,^3J=6.6 Hz, 1H, H11). ^{1}H NMR (400 MHz, $CDCl_3$) δ 133.7 (-NH). ^{13}C NMR (400 MHz, $CDCl_3$) δ 174.0 (C12), 148.0 (C15, C16), 147.6 (C13), 141.6 (C4), 137.0 (C1), 130.0 (C2, C6), 127.3 (C3, C5), 114.2 (C14, C17), 47.8 (C7), 45.0 (C9), 30.1 (C10), 22.4 (C11), 18.1 (C8). ^{11}B NMR (400 MHz, $CDCl_3$) δ −12.7 (m, $-BH_3$). Anal. ($C_{18}H_{22}N_2OBH_3$): Calcd. C, 72.99; H, 8.51; B, 3.65; N, 9.46; O, 5.40; found C, 72.96; H, 8.74; N, 9.28.

2.3.7 | 4-(2-(4-isobutylphenyl) propanamido)-1-methylpyridin-1-ium iodide (3c)

Yellow liquid, 92% yield. ^{1}H NMR (400 MHz, $CDCl_3$) δ 10.91 (-N*H*), 8.48 (d, ^{3} *J*=7.2 Hz, 1H, H15), 8.39 (d, ^3J=7.2 Hz, 1H, H14), 7.39 (^{3}d, ^3J =7.6 Hz, 1H, H2), 7.39 (d, ^3J=7.6 Hz, 1H, H6), 7.0 (d, ^3J=7.6 Hz, 1H, H3), 7.04 (d, ^3J=7.6 Hz, 1H, H5), 4.31 (q, ^3J=6.4 Hz, 1H, H7), 4.20 (s, 1H, -CH_3), 2.33 (d, ^3J=7.2 Hz, 2H, H9), 1.72 (m, 1H, H10), 1.43 (d, ^3J=6.8 Hz, 3H, H8), 0.77 (d, ^3J =6.8 Hz, 6H, H11). ^{15}N NMR (400 MHz, $CDCl_3$) δ 142.6 (-*N*H). ^{13}C NMR (400 MHz, $CDCl_3$) δ 174.7 (C12), 151.8 (C13), 143.9 (C15, C16), 140.0 (C4), 136.5 (C1), 128.5 (C2, C6), 126.8 (C3, C5), 114.4 (C14, C17), 46.7 (C7), 45.6 (N-*C*H3$^+$), 44.0 (C9), 29.1 (C10), 21.4 (C11), 17.8 (C8). Anal. ($[C_{18}H_{22}N_2OCH_3]^+[OH]^-$): Calcd. C, 72.58; H, 8.33; N, 8.91; O, 10.18; found C, 72.49; H, 8.33; N, 8.90.

2.3.8 | 1a′

^{1}H NMR (400 MHz, C_6D_6) δ 9.63 (s, 1H, -NH), 7.40 (d, ^3J=8.7 Hz, 1H, H14), 7.26 (d, ^3J=5.8 Hz 1H, H17),7.05 (d, ^3J=8.7 Hz, 1H, H2), 7.05 (d, ^3J=8.7 Hz, 1H, H6), 6.94 (m, 1H, H15), 6.88 (d, ^3J=8.7 Hz, 1H, H3), 6.88 (d, ^3J=8.7 Hz, 1H, H5), 6.21 (dd, ^3J=6.6 Hz, ^3J=6.6 Hz, 1H, H16), 3.32 (q, ^3J=7.0 Hz, 1H, H7), 2.12 (d, ^3J=7.2 Hz, 2H, H9), 1.51 (m, 1H, H10), 0.61 (d, ^3J=6.6 Hz, 6H, H11). ^{13}C NMR (400 MHz, C_6D_6) δ 172.4 (C12), 148.4 (C13), 143.6 (C17), 141.3 (C4), 136.4 (C1), 136.4 (C15), 130.0 (C2, C6), 127.8 (C3, C5), 119.0 (C16), 117.0 (C14), 48.3 (C7), 44.9 (C9), 30.0 (C10), 21.9 (C11), 17.1 (C8). ^{11}B NMR (400 MHz, C_6D_6) δ 0.4. ^{19}F NMR (400 MHz, C_6D_6) δ −144.7.

2.3.9 | 1b*′

^{1}H NMR (400 MHz, C_6D_6) δ 9.25 (s, 1H, -NH), 8.17 (d, ^3J=8.5 Hz, 1H, H14), 7.08 (d, ^3J=8.0 Hz, 1H, H2), 7.08 (d, ^3J=8.0 Hz, 1H, H6), 7.81 (d, ^3J=5.3 Hz, 1H, H17), 6.77 (m, 1H, H15), 6.77 (d, ^3J=8.0 Hz, 1H, H3), 6.77 (d, ^3J=8.0 Hz, 1H, H5), 5.98 (m,1H, H16), 3.31 (q, ^3J=7.2 Hz, 1H, H7), 2.12 (d, ^3J=6.6 Hz, 2H, H9), 1.51 (m, 1H, H10), 1.25 (d, ^3J=6.8 Hz, 3H, H8), 0.61 (d, ^3J=6.5 Hz, 6H, H11). ^{13}C NMR (400 MHz, C_6D_6) δ 172.3 (C12), 148.7 (C13), 146.1 (C17), 141.5 (C4), 140.6 (C15), 136.9 (C1), 129.9 (C2, C6), 127.5 (C3, C5), 118.1 (C16), 114.9 (C14), 48.3 (C7), 44.8 (C9), 30.1 (C10), 22.6 (C8), 22.6 (C11). ^{11}B NMR (400 MHz, C_6D_6) δ −19.7 (q, $^1J_{(B\text{-}H)}$=106.0 Hz, $-BH_3$).

2.3.10 | 2a′

^{1}H NMR (400 MHz, C_6D_6) δ 9.07 (d, ^3J=5.1 Hz, 1H, H14), 9.07 (s, 1H, -NH), 8.23 (d, ^3J=7.7 Hz, 1H, H17), 8.01 (m, 1H, H15), 7.58 (d, ^3J=8.1 Hz, 1H, H2), 7.58 (d, ^3J=8.1 Hz, 1H, H6), 7.26 (m, 1H, H16), 7.07 (d, ^3J=8.1 Hz, 1H, H3), 7.07 (d, ^3J=8.1 Hz, 1H, H5), 4.11 (q, ^3J=6.4 Hz, 1H, H7), 2.27 (d,^3J=6.2 Hz, 2H, H9), 1.72 (m, 1H, 10H), 1.65 (d, ^3J=6.9 Hz, 3H, H8), 0.75 (d, ^3J=6.6 Hz, 6H, H11). ^{13}C NMR δ (400 MHz, C_6D_6) 175.9 (C12), 141.1 (C4), 138.2 (C1), 137.3 (C13), 136.3 (C14), 135.8 (C15), 132.2 (C16), 129.7 (C2, C6), 127.6 (C3, C5), 127.4 (C17), 47.0 (C7), 44.8 (C9), 30.0 (C10), 22.0 (C11), 17.9 (C8). ^{11}B NMR (400 MHz, C_6D_6) δ −0.2. ^{19}F NMR (400 MHz, C_6D_6) δ −146.5.

2.3.11 | 2b′

^{1}H NMR (400 MHz, C_6D_6) δ 8.44 (s, 1H, H14), 7.66 (d, ^3J=5.7 Hz, 1H, H17), 7.61 (d, ^3J=8.6 Hz, 1H, H15), 7.54 (s, 1H, -NH), 7.11 (d, ^3J=8.0 Hz, 1H, H2), 7.11 (d, ^3J=8.0 Hz, 1H, H6), 6.83 (d, ^3J=8.0 Hz, 1H, H3), 6.83 (d, ^3J=8.0 Hz, 1H, H5), 6.25 (m, 1H, H16), 3.38 (q, ^3J=7.1 Hz, 1H, H7), 2.09 (d, ^3J=7.1 Hz, 2H, H9), 1.51 (m, 1H, H10), 1.32 (d, ^3J=7.0 Hz, 3H, H8), 0.61 (d, ^3J=6.6 Hz, 6H, H11). ^{13}C NMR (400 MHz, C_6D_6) δ 172.8 (C12), 141.5 (C14), 140.9 (C4), 138.0 (C1), 138.8 (C15), 136.8 (C13), 129.7 (C2, C6), 128.5 (C16), 127.0 (C3, C5), 124.9 (C17), 49.7 (C7), 44.9 (C9), 30.1 (C10), 22.6 (C11), 18.8 (C8). ^{11}B NMR (400 MHz, C_6D_6) δ −19.7 (q, $^1J_{(B\text{-}H)}$=105.4 Hz, BH_3).

2.3.12 | 3a′

^{1}H NMR (400 MHz, C_6D_6) δ 9.74 (s, 1H, -NH), 8.06 (w, 1H, H15), 8.06 (w, 1H, H16), 7.78 (w, 1H, H17), 7.78 (w, 1H, H14), 7.41 (d, ^{3}J=8.5 Hz, 1H, H2), 7.41 (d, ^{3}J=8.5 Hz, 1H, H6), 6.95 (d, ^{3}J=7.7 Hz, 1H, H3), 6.95 (d, ^{3}J=7.7 Hz, 1H, H5), 3.96 (m, 1H, H7), 2.11 (d, ^{3}J=6.6 Hz, 2H, H9), 1.53 (m, 1H, H10), 1.36 (d, ^{3}J=6.7 Hz, 3H, H8), 0.58 (d, ^{3}J=6.2 Hz, 6H, H11). ^{13}C NMR (400 MHz, C_6D_6) δ 174.1 (C12), 153.2 (C13), 152.3 (C15, C16), 141.1 (C4), 136.9 (C1), 128.9 (C2, C6), 127.1 (C3, C5), 113.8 (C14, C17), 46.6 (C7), 44.1 (C9), 29.2 (C10), 21.3 (C11), 17.2 (C8). ^{11}B NMR (400 MHz, C_6D_6) δ −0.1. ^{19}F NMR (400 MHz, C_6D_6) δ −147.1.

2.3.13 | 3b′

^{1}H NMR (400 MHz, C_6D_6) δ 7.99 (d, ^{3}J=6.2 Hz, 1H, H15), 7.99 (d, ^{3}J=6.2 Hz, 1H, H16), 7.63 (-NH), 7.24 (d, ^{3}J=7.9 Hz, 1H, H6), 7.24 (d, ^{3}J=7.9 Hz, 1H, H2), 7.09 (d, ^{3}J=6.2 Hz, 1H, H14), 7.09 (d, ^{3}J=6.2 Hz, 1H, H17), 7.01 (d, ^{3}J=7.9 Hz, 1H, H3), 7.01 (d, ^{3}J=7.9 Hz, 1H, H3), 3.68 (q, ^{3}J=6.5 Hz, 1H, H7), 2.29 (d, ^{3}J=6.4 Hz, 2H, H9), 1.74 (m, 1H, H10), 1.51 (w, 3H, H8), 0.84 (d, ^{3}J=6.5 Hz, 1H, H11). ^{13}C NMR (400 MHz, C_6D_6) δ 172.9 (C12), 147.1 (C13), 141.2 (C4), 137.6 (C1), 129.8 (C2, C6), 127.3 (C3, C5), 113.7 (C14, C17), 47.6 (C7), 44.8 (C9), 30.0 (C10), 22.1 (C11), 18.6 (C8), 147.6 (C15, C16). ^{11}B NMR (400 MHz, C_6D_6) δ −19.7 (q, $^{1}J_{(B\text{-}H)}$=106.2 Hz, -BH_3).

2.3.14 | 3c′

^{1}H NMR (400 MHz, C_6D_6) δ 11.38 (-NH), 8.35 (s,1H, H15), 8.30 (s,1H, H14), 8.35 (s,1H, H16), 8.30 (s,1H, H16), 7.85 (d, ^{3}J=7.6 Hz, 1H, H2), 7.85 (d, ^{3}J=7.6 Hz, 1H, H6), 7.12 (d, ^{3}J=8.0 Hz, 1H, H3), 7.12 (d, ^{3}J=8.0 Hz, 1H, H5), 4.75 (q, ^{3}J=6.4 Hz, 1H, H7), 2.31 (d, ^{3}J=8.0 Hz, 2H, H9), 1.73 (m, 1H, H10), 1.59 (d, ^{3}J=6.4 Hz, 3H, H8), 4.13 (s, 3H, -CH_3), 0.82 (d, ^{3}J=6.4 Hz, 6H, H11). ^{13}C NMR (400 MHz, C_6D_6) δ 175.3 (C12), 152.2 (C13), 145.1 (C15, C16), 140.8 (C4), 137.9 (C1), 129.6 (C2, C6), 127.4 (C3, C5), 114.8 (C14, C17), 46.7 (C7), 44.9 (C9), 30.0 (C10), 22.2 (C11), 18.9 (C8).

2.4 | Computational details

Full geometry optimizations were carried out at a density functional theory level using the exchange-correlation hybrid functional B3LYP[32–36] along with the 6-31++G**[37–48] basis set as is implemented in Gaussian 09.[49] A vibrational analysis was performed to discriminate between minima and transition state structures. All calculations were performed using the solvation model based on density, SMD.[50] Computed structures were rendered as images using Chemcraft.[51]

3 | RESULTS AND DISCUSSION

3.1 | NMR analysis of ^{1}H and ^{13}C

The chemical shifts for positions 7, 14-17, and -NH were affected by the adducts formation in both $CDCl_3$ and C_6D_6. The NMR data for ^{1}H and ^{13}C are shown in Tables 2-4. In $CDCl_3$, the amide proton signal in **1a*** and **1b*** is shifted to higher frequencies compared to the raw material (δ-NH **1**: 8.1 ppm; **1a***: 10.24 ppm; **1b***: 9.26 ppm). This change is due to the amide proton's interaction with fluorine and hydride, respectively (Figure 1). Both **1a*** and **1b*** shared a trend in the chemical shifts for 14-17 protons, moving to higher frequencies respect to the raw materials. This is caused by the decrease of electron density on these positions due to the coordination between the pyridine nitrogen and the boron atom. Additionally, the C12 signal in **1a*** appears at higher frequencies (178.8 ppm) than C12 (172.9 ppm) in **1b***. This effect is the result of the noncovalent interaction between the amidic proton and one of the fluorine atoms in **1a***, which allows the carbonyl's electron density to flow to the amide's nitrogen. This is further supported by the ^{15}N NMR data (Table 5).

During the N→BF_3 adduct formation in C_6D_6, two different conformers were observed (**1a*′** and **1a′**). The doubling of the signals in the ^{1}H and ^{13}C NMR spectra confirmed the coexistence of two conformers (see Supporting Information). The second structure differs from **1a*** in the relative position of the BF_3 moiety, which is oriented toward the carbonyl's oxygen (Figure 1, 1a′). The chemical shifts of the carbonyl group (C12) appear at 172.4 and 178.2 ppm for **1a′** and **1a*′**, respectively. Furthermore, two amide protons were observed at 9.63 ppm and 10.45 ppm for **1a′** and **1a*′**, respectively (Table 2).

While structurally similar, the N→BH_3 adduct chemical shifts differ in $CDCl_3$ (**1b***) and C_6D_6 (**1b*′**). For compound **1b*′**, the signals corresponding to protons H14-H17 were shifted to lower frequencies with respect to **1b***. This effect is attributed to weaker Van der Waals interactions between the solvent and the compound, because benzene does not favor these interactions as well as $CDCl_3$. The electronic effects on the C13-C17 positions are similar to those reported for **1a*′**, indicating the formation of the structures shown in Figure 1 (**1b*** and **1b*′**).

The formation of the adducts derived from 3-aminopyridine (**2**) was evidenced by ^{1}H and ^{13}C NMR spectra in $CDCl_3$ and C_6D_6 (Table 3). In general, the most significant changes in ^{1}H NMR spectra are for the amide proton and the H14 position. In all the adducts (**2a**, **2a′**, **2b,** and **2b′**), the H14 signal was shifted to higher frequencies when the aromatic nitrogen's lone electron pair interacts with the boron atom (Figure 2). The amide proton showed a deshielding effect on the N→BF_3 derivatives, an effect that was not observed on the N→BH_3 adducts, where the acidic proton (-NH) was shifted to lower frequencies. On the ^{13}C NMR spectra, all the adducts exhibit

TABLE 2 Selected ^{1}H and ^{13}C NMR shifts (ppm) of **1a-1b** adducts in $CDCl_3$ and C_6D_6 (see Figure 1 for numbering sequence)

	1a*		1b*		1a′		1a*′		1b*′	
	^{1}H	^{13}C	^{1}H	^{13}C	^{1}H	^{13}C	^{1}H	^{13}C	^{1}H	^{13}C
7	3.93	46.9	3.55	48.4	3.32	48.3	4.03	46.3	3.31	48.3
12	—	178.8	—	172.9	—	172.4	—	178.2	—	172.3
13	—	148.4	—	148.8	—	148.4	—	148.0	—	148.7
14	8.21	116.8	8.51	115.5	7.40	117.0	8.19	116.3	8.17	114.9
15	7.56	136.8	7.82	141.5	6.94	136.4	7.15	136.3	6.77	140.6
16	7.38	121.0	7.02	118.8	6.21	119.0	6.37	119.7	5.98	118.1
17	8.16	147.1	8.28	146.5	7.26	143.6	7.92	146.2	7.81	146.1
-NH	10.24	—	9.28	—	9.63	—	10.45	—	9.25	—

(′) Compounds in benzene; (*for cyclic conformer).

TABLE 3 Chemical shifts δ (ppm) of characteristic peaks in the ^{1}H and ^{13}C spectra of *meta* adducts in $CDCl_3$ andC_6D_6

	2a		2a′		2b		2b′	
	^{1}H	^{13}C	^{1}H	^{13}C	^{1}H	^{13}C	^{1}H	^{13}C
7	3.87	46.9	4.11	47.0	3.71	47.5	3.38	49.7
12	—	175.7	—	175.9	—	173.5	—	172.8
13	—	136.2	—	137.3	—	136.9	—	136.8
14	9.11	136.9	9.07	136.3	8.60	138.7	8.44	141.5
15	8.27	136.5	8.01	135.8	8.34	129.4	7.61	138.8
16	7.78	132.5	7.26	132.2	7.39	125.4	6.25	128.5
17	8.47	127.7	8.23	127.4	8.23	142.2	7.66	124.9
-NH	9.11	—	9.05	—	8.05	—	7.54	—

(′)Compounds in benzene.

TABLE 4 Selected chemical shifts δ (ppm) of ^{1}H and ^{13}C spectra of *para* adducts in $CDCl_3$ and C_6D_6

	3a		3a′		3b		3b′		3c		3c′	
	^{1}H	^{13}C	^{1}H	^{13}C	^{1}H	^{13}C	^{1}H	^{13}C	^{1}H	^{13}C	^{1}H	^{13}C
7	3.88	47.4	3.96	46.6	3.80	47.8	3.52	47.6	4.31	46.6	4.75	47.8
12	—	175.5	—	174.1	—	174.0	—	172.9	—	174.7	—	175.3
13	—	141.8	—	153.2	—	147.6	—	147.1	—	151.8	—	152.2
14	8.01	115.0	7.78	113.8	7.62	114.2	7.09	113.7	8.39	114.4	8.30	114.8
15	8.27	153.8	8.06	152.3	8.29	148.0	7.99	147.6	8.48	143.9	8.35	145.1
16	8.27	153.8	8.06	152.3	8.29	148.0	7.99	147.6	8.48	143.9	8.35	145.1
17	8.01	115.0	7.78	113.8	7.62	114.2	7.09	113.7	8.39	114.4	8.30	114.8
-NH	9.31	—	9.74	—	8.24	—	7.63	—	10.91	—	11.38	—

(′)Compounds in benzene.

a deshielding effect for C15 and C16, while C14 and C17 presented a shielding effect because of the activation of the *ortho* and *para* positions of the aromatic ring by the N→B adduct formation (see Supporting Information).

In general, the 4-aminopyridine derivatives of NMR of ^{1}H and ^{13}C spectra showed the same trends for positions 13-17 in both solvents. The formation of the N→BF_3, N→BH_3 adducts, and the covalent bond N-CH_3^+ with the pyridine's

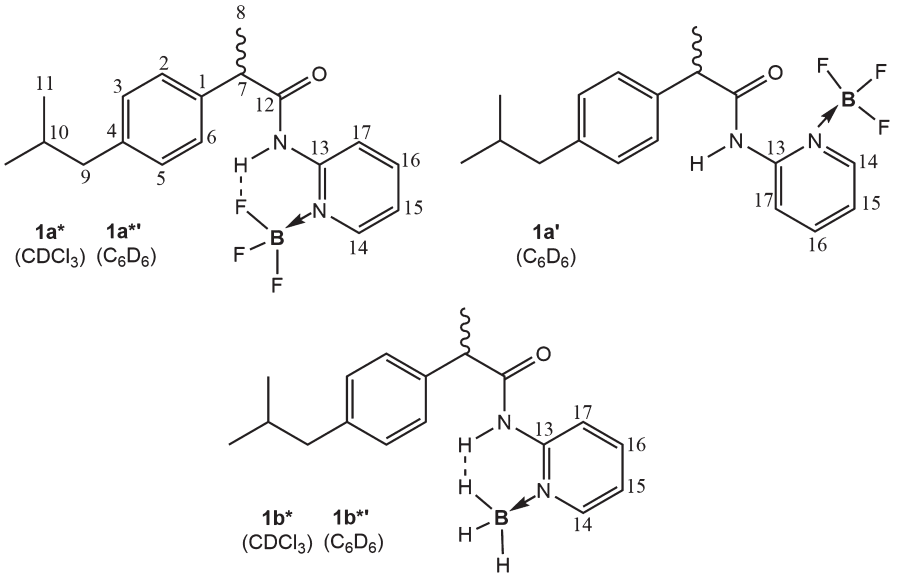

FIGURE 1 Adducts of amide **1** with BF_3 and BH_3 in $CDCl_3$ and C_6D_6

TABLE 5 Chemical shifts (δ) in ppm for ^{11}B, ^{15}N, and ^{19}F in $CDCl_3$

	^{11}B	^{15}N	^{19}F	No.	^{11}B	^{15}N	No.	^{15}N
1a*	−1.0	131.9	−147.8	**1b***	−20.2	136.8	**3c**	142.6
2a	−0.8	126.3	−147.3	**2b**	−20.3	130.6		
3a	−0.9	137.9	−147.2	**3b**	−12.7	133.7		

NMR of ^{15}N was obtained by INEPT. ^{15}N: **1**, 141.3; **2**, 125.2; **3**, 137.2.

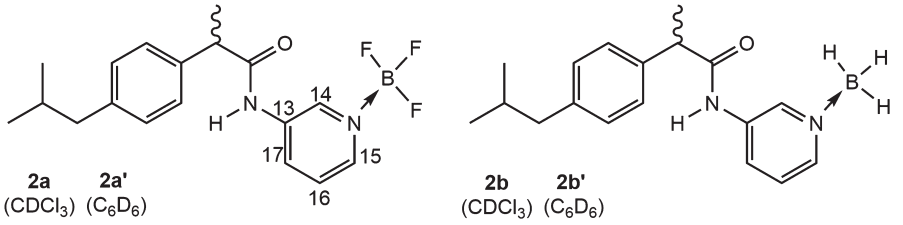

FIGURE 2 Adducts of the amide **2** with BF3 and BH3 in CDCl3 and C_6D_6. The same structure was observed in C_6D_6

nitrogen protects the 15 and 16 positions of the pyridine ring while deshielding the positions 14 and 17 (Table 3). Although the electron distribution trends are the same for **3a**, **3b,** and **3c**, the latter system showed the most significant changes due to the presence of a covalent bond with an electron density donor group. The proposed structures for **3** derivatives are shown in Figure 3. There is an isolobal analogy between these systems, that is, they are isoelectronic because all of them presented the same electronic changes on the pyridine ring, either in the presence of N→B adducts or with the N-C covalent bond.

3.2 | NMR analysis of ^{11}B, ^{15}N and ^{19}F

The analysis of the chemical shifts for the heteroatoms corroborates the behavior of the amides in the adducts formation, and also provides important information about their chemical environment (Table 5). A shielding effect was observed on the amide's nitrogen on the 2-aminopyridine derivatives (**1a*** and **1b***). This results from an increased electron density around the amide nitrogen due to the formation of additional cycles (see Figure 3). For 3-aminopyridine derivatives, a slight deshielding effect on the amide's nitrogen was observed on **2b**. This indicates that the adduct formation on this position does not affect the electron density around this atom. A completely different behavior was observed on **3a**, **3b,** and **3c**, where the signal of ^{15}N was shifted to higher frequencies because the pyridine nitrogen is at a *para* position respect to the amide moiety.

The ^{11}B NMR signals were analyzed and compared with other reported systems, expecting the BF_3 and BH_3 chemical shifts in the range of −0.9 to −11.5 ppm, for the compounds where the boron atom is coordinated with the pyridine's nitrogen.[52] The **1b*** compound shows a quartet signal at −20.2 ppm with a coupling constant $^1J_{(B\text{-}H)}$=105.5 Hz, characteristic of an N→BH_3 coordination. In the case of **1b*′,**

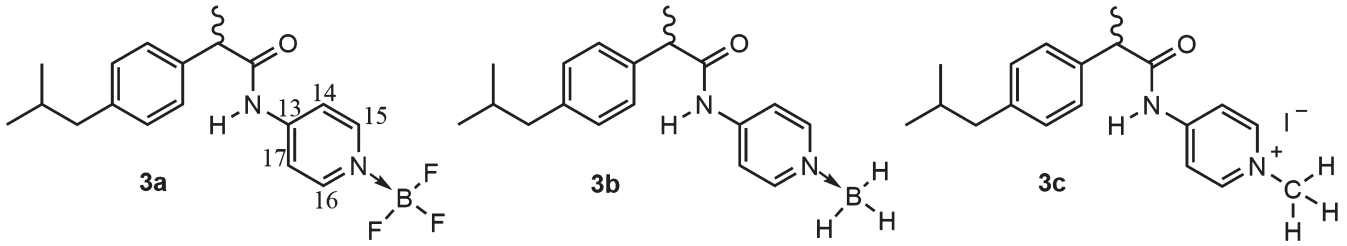

FIGURE 3 Adducts of **3** with BF_3, BH_3, and CH_3I in $CDCl_3$. The same structure was observed in C_6D_6

the ^{11}B signal appears at −19.7 ppm, confirming the adduct formation. For the **2b** adduct, a quartet signal was observed at −20.3 ppm with a $^1J_{(B\text{-}H)}$=106.3 Hz, confirming the formation of the N→B adduct with the pyridine nitrogen. Finally, a quartet signal at −20.1 ppm for **2b′**.

The signal for ^{19}F appears at lower frequencies with respect to the reagent ($Et_2O{\cdot}BF_3$, −127 ppm), due to the exchange of the oxygen for the nitrogen on the boron atom.

3.3 | Conformational analysis of the amide 1a in chloroform and benzene

To further explain the proposed structures for N→BF_3 and N→BH_3 adducts in chloroform and benzene, quantum chemical calculations were performed. A conformational search for the above compounds using *Gaussian09* code was performed. The geometry optimization of molecule **1a*** under the solvent effect of chloroform only identified one conformer (Figure 4) as a minimum on the potential energy surface.

In contrast to chloroform, two conformers were found for the same molecule using benzene as solvent (Figure 5). The Gibbs free energy difference between the structures was 9.624 kcal/mol. This finding together with the rotational pathway between both conformers supports their coexistence, as observed in the NMR data.

For **1b***, a similar structure was found, where the amide and pyridine orientations were analogous to those observed on **1a***. The main difference between **1a*** and **1b*** is the orientation of the boron's substituents. While in **1a***, a single fluorine interacts with the amide's proton, **1b*** has two hydrides forming an asymmetric bifurcate interaction with the corresponding proton (Figure 6). This structural arrangement supports the chemical shifts discussed in the NMR section.

3.4 | Infrared analysis

The characteristic bands of stretching for amide carbonyl group ν(C=O) appear between 1695 and 1620 cm^{-1}, near of C=N stretching bands (1590-1510 cm^{-1}). In the amide bands, stretching for C-N bond is a strong signal around 1480-1410 cm^{-1} and N-H asymmetric and symmetric stretching appear a broad signal at 3350-3150 cm^{-1}. Stretching N-H band gives us important information about the chemical environment surrounding to the acid proton. Selected IR stretching bands for the amine-borane adducts and N-CH_3^+ bond are presented in Table 6.

The difference between the asymmetric and symmetric stretching of the N-H bonds for **1a** is 18 cm^{-1}, while it is 69 cm^{-1} for **2a** and 37 cm^{-1} for **3a**. This phenomenon is related to the proton-fluorine (N-$H^+\cdots{}^-$F-B) interaction in **1a**. The splitting of signals in **2a** was attributed to the distance between the proton and fluorine in addition to the steric hindrance that apparently inhibits any intermolecular interaction for the amide's proton. Contrastingly, this splitting disappears in **1b**, **3b,** and **3c**, where a single broad band was observed. Changes in N-H stretching vibrations are related with the coordination of this proton with electron donor atoms. This changes are attributed to hydride-proton interactions which inhibit the splitting of the bands in **1b**, which generates enhanced structural stability (N-$H^+\cdots{}^-$H-B). This is further supported by the movement of the chemical shift for the N-H proton at higher frequencies in NMR. The formation of the

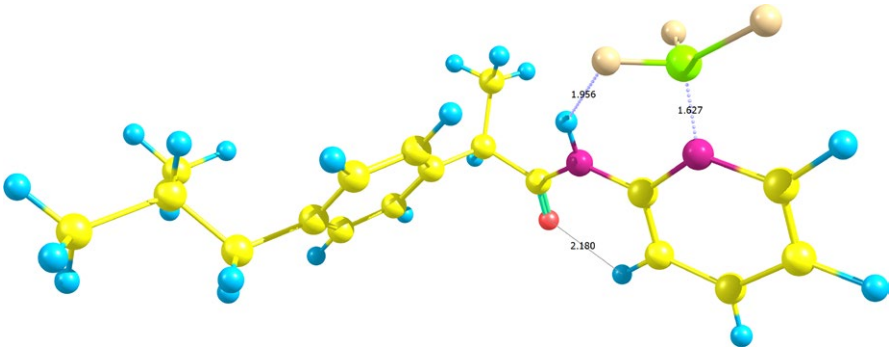

FIGURE 4 Structural rearrangement of amide **1a*** in chloroform

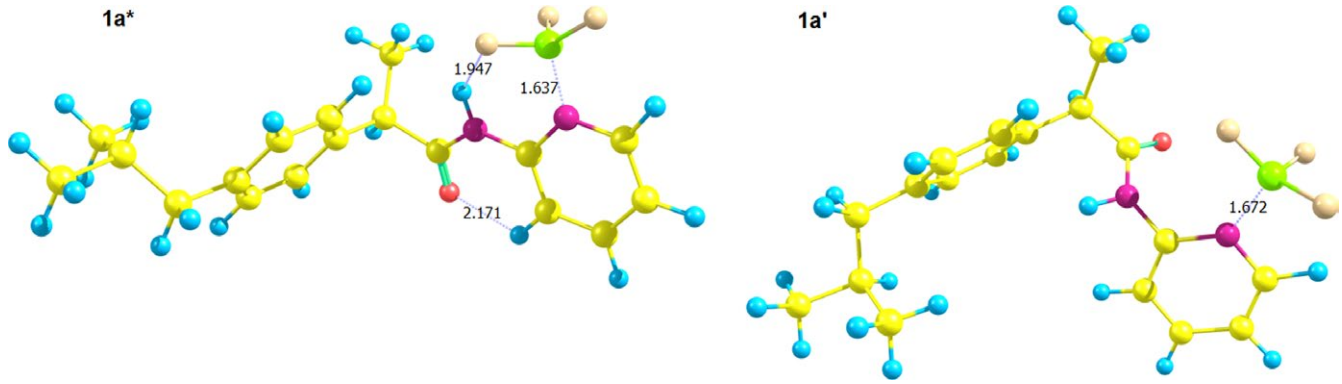

FIGURE 5 Structural rearrangements of the amide **1** with BF_3 in benzene

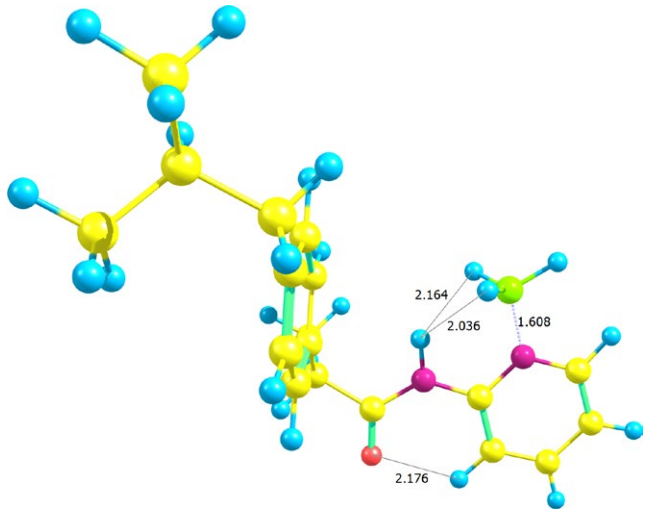

FIGURE 6 Structural rearrangements of the amide **1b**

$N\rightarrow BX_3$ adducts is supported by the appearance of a strong band at 1160-1140 cm^{-1} due to the N-B stretching for these ligands.[53,54] The **1a**, **2a,** and **3a** adducts exhibited a broad and strong band at 1100-1000 cm^{-1}, because of the B-F symmetric and asymmetric stretching.[55] As it is known, the B-H stretching appears at 2400-2200 cm^{-1}, as a broad band of medium intensity, where higher frequencies correspond to the free hydride ($N\rightarrow BH_3$) and the lower frequencies are caused by the hydrides coordinated with the amide proton ($N\text{-}H^{+}\cdots{}^{-}H\text{-}B$).[56,57]

4 | CONCLUSIONS

Amine-borane adducts ibuprofen derivatives have been successfully developed. The analyses of IR, NMR (^{1}H, ^{11}B, ^{13}C, ^{15}N, and ^{19}F) data, and DFT calculations demonstrated that $N\rightarrow BX_3$ adducts were formed on pyridine ring.

The 2-aminopyridine derivatives (**1a*** and **1b***) formed cycles between the amide proton and the hydride and fluorine, which acted as donors in the $N\text{-}H^{+}\cdots{}^{-}X\text{-}B$ intramolecular interactions. Another cycle was observed on these structures, formed by the interaction of the carbonyl's oxygen and a pyridine's hydrogen. The duplication of the carbonyl chemical shift in the NMR spectrum for the $N\rightarrow BF_3$ complex in benzene indicates the presence of a second coexisting structure (**1a′**), where the previously discussed cycles were not formed.

DFT calculations showed a connecting path between structures **1a*′** and **1a′**, through the rotation of the amide-pyridine

TABLE 6 Characteristic infrared bands of ibuprofen amides in $N\rightarrow BH_3$, $N\rightarrow BF_3$ adducts, and $N\text{-}CH_3^{+}$ bond

	Wavenumber (cm^{-1})							
No.	**ν(C=O)**	**ν(C=N) (pyridine)**	**ν(C-N) (amide)**	**ν_a(N-H)**	**ν_s(N-H)**	**ν(B-N)**	**ν_a(B-X) (X=H or F)**	**ν_s(B-X) (X=H or F)**
1a	1652 (s)	1572 (s)	1439 (s)	3270(b)	3252 (b)	1155 (s)	1090 (b,s)	999 (b,s)
2a	1630 (w)	1544 (s)	1459 (s)	3343 (b)	3274 (b)	1160 (m)	1056 (b,s)	1020 (b,s)
3a	1639 (m)	1506 (s)	1477 (s)	3322 (b)	3285 (b)	1142 (m)	1051 (b,s)	1020 (b,s)
1b	1623 (m)	1511 (s)	1438 (s)	3311 (b)		1148 (m)	2397 (m), 2310 (m)	
2b	1628 (m)	1508 (s)	1432 (s)	3322 (b)	3290 (b)	1149 (s)	2359 (m), 2308 (m), 2276 (m)	
3b	1674 (m)	1538 (s)	1428 (s)	3311 (b)		1154 (s)	2368 (m), 2267 (m)	
3c	1641 (m)	1517 (s)	1432 (m)	3422 (b)				

a, X=H; b, X= F; s, strong; m, medium; w, weak; b, broad.

bond. The calculated Gibbs free energies showed a difference of 9.624 kcal/mol between the structures, with **1a*** having the lower energy. These computational results support the coexistence of both conformers.

The NMR analyses of the **3a**, **3b,** and **3c** systems in both solvents present the same chemical shift trend between them, where the *ortho* and *para* positions were shielding, while that *meta* was deshielding. This confirms an isolobal analogy between the N-C and N→B interactions in these compounds.

ACKNOWLEDGMENTS

Maria Romero-Chávez is grateful for the scholarship 289752 from CONACYT-México and partial funding support by grant #130381 and grant #226165 provided by CONACYT are also acknowledged. Magaña-Vergara Nancy E. and the University of Colima are thankful for the scholarship to SEP-PRODEP.

REFERENCES

[1] S. Hekmanek, *Chem. Rev.* **1992**, *92*, 325.
[2] A. Flores-Parra, R. Contreras, *Coord. Chem. Rev.* **2000**, *196*, 85.
[3] C. D. Hunt, *J. Trace Elem. Med Biol.* **2012**, *26*, 157.
[4] N. A. Bakken, C. D. Hunt, *J. Nutr.* **2003**, *132*, 3516.
[5] F. H. Nielsen, B. J. Stoecker, *Trace Elem. Med. Biol.* **2009**, *23*, 195.
[6] C. D. Hunt, J. L. Herbel, J. P. Idso, *J. Bone Miner. Res.* **1994**, *9*, 171.
[7] S. L. Meacham, L. J. Taper, S. L. Volpe, *Am. J. Clin. Nutr.* **1995**, *61*, 341.
[8] C. D. Hunt, J. L. Herbel, F. H. Nielsen, *Am. J. Clin. Nutr.* **1997**, *65*, 803.
[9] T. Armstrong, J. W. Spears, T. D. Crenshaw, F. H. Nielsen, *J. Nutr.* **2000**, *130*, 2575.
[10] D. J. Fort, E. L. Stover, R. L. Rogers, H. F. Copley, L. A. Morgan, E. R. Foster, *Biol. Trace Elem. Res.* **2000**, *77*, 173.
[11] M. Kuangbiao, M. Scheibitz, S. Scholz, M. Wagner, *J. Organomet. Chem.* **2002**, *652*, 11.
[12] J. Lalevée, M. A. Tehfe, X. Allonas, J. P. Fourassier, *Macromolecules* **2008**, *41*, 9057.
[13] J. R. Vance, A. Schäfer, A. P. Robertson, K. Lee, J. Turner, G. R. Whittell, I. Manner, *J. Am. Chem. Soc.* **2014**, *136*, 3048.
[14] A. Staubitz, A. P. Robertson, I. Manners, *Chem. Rev.* **2010a**, *110*, 4079.
[15] A. Staubitz, A. P. Robertson, M. E. Sloan, I. Manners, *Chem. Rev.* **2010b**, *110*, 4023.
[16] H. Zhang, C. Huo, K. Ye, P. Zhang, W. Tian, Y. Wang, *Inorg. Chem.* **2006**, *45*, 2788.
[17] B. L. Conley, D. Guess, T. J. Williams, *J. Am. Chem. Soc.* **2011**, *133*, 14212.
[18] A. D. Sutton, A. K. Burrel, D. A. Dixon, E. B. I. I. I. Garner, J. C. Gordon, T. Nakagawa, K. C. Ott, J. P. Robinson, M. Vasiliu, *Science* **2011**, *331*, 1426.
[19] A. Ariza-Castolo, M. A. Paz-Sandova, R. Contreras, *Magn. Reson. Chem.* **1992**, *30*, 520.
[20] J. C. Gálvez-Ruiz, E. Solano-Ruiz, S. A. Sánchez-Ruiz, R. Contreras, A. Flores-Parra, *ARKIVOC* **2008**, 81.
[21] L. M. Engelhardt, G. E. Jacobsen, P. C. Junk, C. L. Raston, A. H. Whitea, *J. Chem. Soc. Chem. Commun.* **1990**, *1*, 89.
[22] J. A. Joule, K. Mills, Heterocyclic Chemistry, John Wiley & Sons, Chichester, UK **2010**.
[23] M. Allegretti, R. Bertini, M. C. Cesta, C. Bizzarri, R. Di Bitondo, V. Di Cioccio, E. Galliera, V. Berdini, A. Topai, G. Zampella, V. Russo, N. Di Bello, G. Nano, L. Nicolini, M. Locati, P. Fantucci, S. Florio, F. Colotta, *J. Med. Chem.* **2005**, *48*, 4312.
[24] F. Sagan, R. Filas, M.P. Mitoraj, *Crystals* **2016**, *6*, 28.
[25] C. Reichardt, T. Welton, Solvents and Solvent Effects in Organic Chemistry, Wiley-VCH, Weinheim, Germany **2011**.
[26] D. J. Wolstenholme, E. J. Fradsham, G. S. McGrady, *CrystEngComm* **2015**, *17*, 7623.
[27] M. M. Faisal, A. H. Najeh, *Pharmaceuticals* **2012**, *5*, 1080.
[28] M. T. Cocco, C. Congiu, V. Onnis, M. Morelli, O. Cauli, *Eur. J. Med. Chem.* **2003**, *38*, 513.
[29] A. Krzyzaniak, M. Leeman, F. Vossebeld, T. J. Visser, B. Schuur, A. B. Haan, *Sep. Purif. Technol.* **2013**, *111*, 82.
[30] V. Diemer, H. Chaumeil, A. Defoin, A. Fort, A. Boeglin, C. Carré, *Eur. J. Org. Chem.* **2006**, 2727.
[31] H. Chaumeil, P. Jacques, V. Diemer, D. Le Nouën, C. Carré, *Eur. J. Org. Chem.* **1002**, *2011*, 70.
[32] S. H. Vosko, L. Wilk, M. Nusair, *Can. J. Phys.* **1980**, *58*, 1200.
[33] C. Lee, W. Yang, R. G. Parr, *Phys. Rev. B* **1998**, *37*, 785.
[34] A. D. Becke, *Phys. Rev. A* **1998**, *38*, 3098.
[35] A. D. Becke, *J. Chem. Phys.* **1993**, *98*, 5648.
[36] B. Miehlich, A. Savin, H. Stoll, H. Preuss, *Chem. Phys. Lett.* **1989**, *157*, 200.
[37] R. Ditchfield, W. J. Hehre, J. A. Pople, *J. Chem. Phys.* **1971**, *54*, 724.
[38] W. J. Hehre, R. Ditchfield, J. A. Pople, *J. Chem. Phys.* **1972**, *56*, 2257.
[39] J. A. Pople, P. C. Hariharan, *Theor. Chem. Acc.* **1973**, *28*, 213.
[40] J. A. Pople, P. C. Hariharan, *Mol. Phys.* **1974**, *27*, 209.
[41] M. S. Gordon, *Chem. Phys. Lett.* **1980**, *76*, 163.
[42] M. M. Francl, W. J. Pietro, W. J. Hehre, J. S. Binkley, D. J. DeFrees, J. A. Pople, M. S. Gordon, *J. Chem. Phys.* **1982**, *77*, 3654.
[43] T. Clark, J. Chandrasekhar, G. W. Spitznagel, P. Schleyer, *J. Comp. Chem.* **1983**, *4*, 294.
[44] R. C. Binning, L. A. Curtiss, *J. Comp. Chem.* **1990**, *11*, 1206.
[45] J. P. Blaudeau, M. P. McGrath, L. A. Curtiss, L. Radom, *J. Chem. Phys.* **1997**, *107*, 5016.
[46] M. J. Frisch, J. A. Pople, J. S. Binkley, *J. Chem. Phys.* **1984**, *80*, 3265.
[47] V. A. Rassolov, J. A. Pople, M. A. Ratner, T. L. Windus, *J. Chem. Phys.* **1998**, *109*, 1223.
[48] V. A. Rassolov, M. A. Ratner, J. A. Pople, P. C. Redfern, L. A. Curtiss, *J. Comp. Chem.* **2001**, *22*, 976.
[49] M. J. Frisch, G. W. Trucks, H. B. Schlegel, G. E. Scuseria, M. A. Robb, J. R. Cheeseman, G. Scalmani, V. Barone, B. Mennucci, G. A. Petersson, H. Nakatsuji, X. Li, H. P. Hratchian, A. F. Izmalov, J. Bloino, G. Zheng, J. L. Sonnenberg, M. Hada, M. Ehara, K. Toyota, R. Fukuda, J. Hasegawa, M. Ishida, T. Nakajima, Y. Honda, O. Kitao, H. Nakai, T. Vreven, J. A. Montgomery, J. E. Peralta, F. Ogliaro, M. Bearpark, J. J. Heyd, E. Brothers, K. N. Kudin, V. N. Staroverov, R. Kobayashi, J. Normand, K. Raghavachari, A. Rendell, J. C. Burant, S. S. Iyengar, J. Tomasi, M. Cossi, N. Rega, J. M. Millam, M. Klene, J. E. Knox, J. B.

Cross, V. Bakken, C. Adamo, J. Jaramillo, R. Gomperts, R. E. Stratmann, O. Yazyev, A. J. Austin, R. Cammi, C. Pomelli, J. W. Ochterski, R. L. Martin, K. Morokuma, V. G. Zakrzewski, G. A. Voth, P. Salvador, J. J. Dannenberg, S. Dapprich, A. D. Daniels, O. Farkas, J. B. Foresman, J. V. Ortiz, J. Cioslowski, D. J. Fox, Gaussian 09, Gaussian Inc, Wallingford CT **2009**.

[50] A. V. Marenich, C. J. Cramer, D. G. Truhlar, *J. Phys. Chem. B* **2009**, *113*, 6378.

[51] G. A. Adrienko; I. N. Senchenya. http://www.chemcraftprog.com.

[52] T. P. Onak, H. Landesman, R. E. Willams, I. J. Shapiro, *Phys. Chem.* **1959**, *63*, 1533.

[53] L. J. Bellamy, W. Gerrard, M. F. Lappert, R. L. William, *J. Chem. Soc.* **1985**, *58*, 2412.

[54] J. D. Odom, J. A. Barnes, B. A. Hudgens, J. R. Durig, *J. Phys. Chem.* **1974**, *78*, 1503.

[55] G. M. Begund, A. A. Palko, *J. Chem. Phys.* **1963**, *38*, 2112.

[56] L. M. Epstein, E. S. Shubina, E. V. Bakhmutova, L. N. Saitkulova, V. I. Bakhmutov, A. L. Chistyakov, I. V. Stankevich, *Inorg. Chem.* **1998**, *37*, 3013.

[57] C. Merten, C. J. Berger, R. McDonald, Y. Xu, *Angew. Chem. Int. Ed.* **2014**, *53*, 9940.

SUPPORTING INFORMATION

Additional Supporting Information may be found online in the supporting information tab for this article.

How to cite this article: Romero-Chávez MM, Pineda-Urbina K, Magaña-Vergara NE, Vázquez-Cárdenas R, Gómez-Sandoval Z, Ramos-Organillo Á. Conformational analysis of N→BH_3, N→BF_3, and N-CH_3^+ complexes with ibuprofen-derivative amides. *Heteroatom Chem*. 2017;00:e21368. https://doi.org/10.1002/hc.21368